

## Exploring the boundaries of the nuclear landscape: $\alpha$ -decay properties of $^{211}\text{Pa}$

K. Auranen<sup>1,\*</sup>, J. Uusitalo<sup>1</sup>, H. Badran<sup>1,†</sup>, T. Grahn<sup>1</sup>, P. T. Greenlees<sup>1</sup>, A. Herzán<sup>1,2</sup>, U. Jakobsson<sup>1</sup>, R. Julin<sup>1</sup>, S. Juutinen<sup>1</sup>, J. Konki<sup>1</sup>, M. Leino<sup>1</sup>, A.-P. Leppänen<sup>3</sup>, G. O'Neill<sup>1,4,‡</sup>, J. Pakarinen<sup>1</sup>, P. Papadakis<sup>1,§</sup>, J. Partanen<sup>1,||</sup>, P. Peura<sup>1</sup>, P. Rahkila<sup>1</sup>, P. Ruotsalainen<sup>1</sup>, M. Sandzelius<sup>1</sup>, J. Sarén<sup>1</sup>, C. Scholey<sup>1,¶</sup>, L. Sinclair<sup>1,5</sup>, J. Sorri<sup>1,†</sup>, S. Stolze<sup>1,#</sup> and A. Voss<sup>1</sup>

<sup>1</sup>University of Jyväskylä, Department of Physics, P.O. Box 35, FI-40014 University of Jyväskylä, Finland

<sup>2</sup>Institute of Physics, Slovak Academy of Sciences, SK-84511 Bratislava, Slovakia

<sup>3</sup>Radiation and Nuclear Safety Authority – STUK, Lähteentie 2, 96400, Rovaniemi, Finland

<sup>4</sup>University of Liverpool, Department of Physics, Oliver Lodge Laboratory, Liverpool L69 7ZE, United Kingdom

<sup>5</sup>Department of Physics, University of York, Heslington, York, YO10 5DD, United Kingdom



(Received 23 June 2020; accepted 17 August 2020; published 3 September 2020)

Employing the recoil ion transport unit (RITU) and a fusion-evaporation reaction, the  $\alpha$  decay of  $^{211}\text{Pa}$  has been identified via the implantation-decay correlation technique through observation of chains up to four consecutive decays. An  $\alpha$ -particle energy and half-life of 8320(40) keV and  $3.8^{+4.6}_{-1.4}$  ms, respectively, were measured, corresponding to favored  $\alpha$  decay. In addition, more precise  $\alpha$ -decay properties of  $^{212}\text{Pa}$  and  $^{213}\text{Pa}$  were obtained due to accumulated statistics. The present data were compared to those predicted by selected atomic mass models and it was used to estimate the possibility of observing proton emission from these isotopes.

DOI: [10.1103/PhysRevC.102.034305](https://doi.org/10.1103/PhysRevC.102.034305)

### I. INTRODUCTION

At the end of the calendar year 2019, a total of 3308 nuclides had been identified [1]. Out of these 284 stable [2] (or essentially stable<sup>1</sup>) nuclei form a valley of stability at the center of the nuclear landscape. Any deviation from this valley leads to territory associated with radioactive decay. Most commonly, these nuclei morph via  $\alpha$  or  $\beta$  particle emission, or they disintegrate in the process of nuclear fission, but more exotic decay modes are also known. The stability of the nucleus is primarily determined by the energy needed to remove a nucleon, and once this quantity becomes negative a dripline has been reached. In other words, beyond the dripline the binding energy of the nucleus is not sufficient to keep the outermost nucleons in the proximity of the nuclear core, but instead a swift particle emission might occur. On the proton-rich side of the nuclear chart a proton(s) might tunnel through

the Coulomb barrier, leading to a one (two) proton emission, and thus, a proton dripline (two-proton dripline) is formed. In contrast, on the opposite extreme of the Segré chart, a neutron dripline exist beyond which neutron(s) are promptly emitted as those are transparent to the Coulomb force. Nuclear density functional theory [3] anticipates that altogether 6900(500) nuclei with  $Z \leq 120$  are sandwiched between these driplines. The nuclei in the proximity of the driplines provide fundamental information on the properties of the nuclear matter with extreme proton-neutron ratios. Additionally, elements heavier than iron are forged in fierce stellar processes such as the rapid proton capture ( $rp$  process [4–6]) in binary systems involving a neutron star, and the rapid neutron capture process ( $r$  process [7]) taking place in core-collapse supernovae and neutron star mergers [8]. The  $rp$  process ( $r$  process) is thought to proceed in the proximity of the proton (neutron) dripline, hence, understanding the properties of the most exotic nuclei is crucial in order to characterize the path of these stellar explosions, and the abundance of the elements in the universe.

Perhaps the longest standing issue in experimental low-energy nuclear physics is to map the boundaries of the nuclear chart. These experiments, however, are exceptionally challenging owing to the minuscule production yields and short half-lives of nuclei near the dripline. While the proton-rich boundary has been experimentally reached up to neptunium (element 93) [9], the neutron dripline has been characterized only up to neon (element 10) [10]. The next generation radioactive ion beam facilities, like FAIR [11], FRIB [12], and RIBF [13], are expected to significantly infiltrate into the neutron-rich “Terra Incognita”, yet these facilities are still at least a few years away from full operation. Therefore, the only dripline nuclei reachable over a significant mass range with the techniques available to date are those on the proton-rich side. The heaviest proton-dripline nuclei typically disintegrate

\*kalle.e.k.auranen@jyu.fi

<sup>†</sup>Present address: Radiation and Nuclear Safety Authority – STUK, Laippatie 4, 00880 Helsinki, Finland.

<sup>‡</sup>Present address: Department of Physics, University of York, Heslington, York, YO10 5DD, United Kingdom.

<sup>§</sup>Present address: STFC Daresbury Laboratory, Daresbury, Warrington WA4 4AD, United Kingdom.

<sup>||</sup>Deceased.

<sup>¶</sup>Present address: MTC Limited, Ansty Park, Coventry CV79JU, United Kingdom.

<sup>#</sup>Present address: Physics Division, Argonne National Laboratory, 9700 South Cass Avenue, Lemont, Illinois 60439, USA.

<sup>1</sup>Here, we consider a nucleus to be essentially stable if it has a half-life greater than, or comparable to, the age of the solar system, i.e., greater than  $1 \times 10^9$  y.

via emission of an  $\alpha$  particle. Observing the characteristic  $\alpha$  radiation provides a clean and precise way to identify the most neutron-deficient isotopes (see, for example, Refs. [14–16]) and the heaviest elements (Refs. [17,18]). The cleanliness of the decay signal can be further enhanced by correlating the  $\alpha$  decay of the mother nucleus to those of the daughter species. This method allows studies where the number of events is exceptionally low. Even with low statistics one can still probe the fundamental properties of nuclei, for instance their mass. By measuring the energy released in the decay process  $Q_\alpha$ , combined with a knowledge of the mass of the daughter nucleus and the  $\alpha$  particle, the mass of the decaying isotope can be deduced. Masses extracted this way are rough compared to the state-of-the-art precise mass studies, like the Penning trap or the multireflection time-of-flight experiments, but nevertheless those allow us to address important questions, such as (i) testing of advanced atomic mass formulae and their predictive power, (ii) characterization of the one and two proton driplines, and prediction of new cases of one and two proton disintegration, (iii) testing the existence of Thomas-Ehrman shift [19,20] in heavy nuclei, and (iv) testing the strength of the known and predicted shell closures on nuclei far from  $\beta$  stability. Furthermore, the  $\alpha$ -decay rate provides insight on the preformation of the  $\alpha$  particle inside the mother nucleus, but also on the underlying nuclear structure, i.e., on the overlap of the initial and final state wave functions.

The element 91, initially referred as  $\text{UrX}_2$ , was discovered in 1913 by Fajans and Göhring via observation of  $^{234}\text{Pa}$  [21], followed by the independent discovery of  $^{231}\text{Pa}$  by Soddy and Cranston<sup>2</sup> [23] and Hahn and Meitner [24] in 1918, of which the latter initiated the name protactinium [25]. To date, 28 protactinium isotopes, with a mass number ranging from 212 to 239, have been rigorously identified [2,25]. Many attempts have been taken to expand the nuclear horizon beyond these isotopes. In Ref. [26] Yang *et al.* tried to produce and identify  $^{211}\text{Pa}$  via a fusion-evaporation reaction and a recoil separator, but no candidate events were recorded. Nearly a decade earlier, a different approach employing a fragmentation reaction was chosen by Kurcewicz *et al.* [27]. A few candidate events for  $^{211}\text{Pa}$  were observed, but as the authors of Ref. [27] put it “the statistics and the resolution of the ion identification procedure at this setting were not sufficient to claim unambiguous observation of these [ $^{208}\text{Th}$  and  $^{211}\text{Pa}$ ] isotopes”. Furthermore, the decay properties of  $^{211}\text{Pa}$  were not addressed in Ref. [27].

In this article we provide the first rigorous evidence of the existence of the beyond-proton dripline nucleus  $^{211}\text{Pa}$ . This was achieved by correlating a recoil-implantation event with up to four generations of subsequent  $\alpha$ -decay events occurring in the same pixel of the implantation detector. Searching for such recoil-decay correlations is known to be an extremely selective method, and therefore suitable for studies involving the weakest production channels, like the one for  $^{211}\text{Pa}$  for which we measured a notably low cross section of approximately 20 pb. In addition, we report the  $\alpha$ -decay

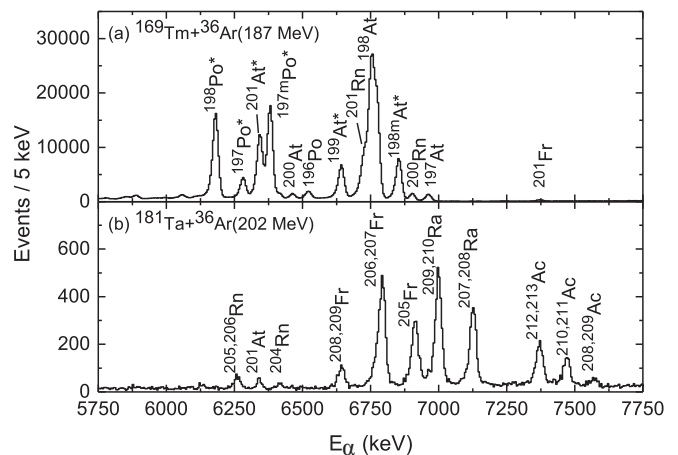


FIG. 1. (a) MWPC vetoed  $\alpha$ -particle energy spectrum obtained during a calibration run. Activities marked with an asterisk were used to gainmatch the individual strips of the DSSD. (b) Energy spectrum of the recoil-correlated  $\alpha$  particles recorded during phase 5 (see Table I) of the experiment.

properties of  $^{211}\text{Pa}$  together with a discussion addressing, but not limited to, the fundamental questions (i)–(iii) summarized above. As  $^{211}\text{Pa}$  is far from known  $Z = 82$  and  $N = 126$  shell closures we do not address question (iv) here, although some relativistic mean-field calculations [28,29] anticipated a nearby proton-shell closure at  $Z = 92$ . In contrast, large-scale shell-model calculations [30] and density-dependent Hartree Fock theory with  $\rho$ -tensor coupling [31] together with multiple experimental work [9,32,33] have shown that there is no proton-shell closure at  $Z = 92$ .

## II. EXPERIMENT

The  $^{181}\text{Ta}(^{36}\text{Ar}, 6n)^{211}\text{Pa}$  fusion-evaporation reaction was chosen to produce the nuclei of interest, but also events arising from the  $5n$  ( $^{212}\text{Pa}$ ) and  $4n$  ( $^{213}\text{Pa}$ ) evaporation channels were observed. An alternate attempt using the reaction  $^{159}\text{Tb}(^{56}\text{Fe}, xn)^{215-x}\text{Pa}$  was made, but no  $\alpha$ -decay chains associated with the protactinium isotopes were recorded with this reaction mainly due to lower primary beam intensities. Furthermore, a separate calibration data set, displayed in Fig. 1(a), was collected with a  $^{36}\text{Ar} + ^{169}\text{Tm}$  reaction in order to gainmatch the individual strips of the implantation detector, which is described later in this section. The ion beams were delivered by the K-130 cyclotron of the University of Jyväskylä with the beam energies and intensities listed on Table I. The recoil ion transport unit (RITU) gas-filled recoil separator [34,35] was used to filter the fusion-evaporation residues, referred to as recoils hereafter, from the flux of the primary beam and other unwanted target and beam-like particles. At the focal plane of RITU the recoils were identified based on their energy loss in a multiwire proportional counter (MWPC) and on the time-of-flight between the MWPC and the subsequent implantation detector of the GREAT spectrometer [36]. A high granularity double-sided silicon strip detector (DSSD), with a  $1\text{ mm}^2$  pixel size and a thickness of  $300\ \mu\text{m}$ , was used to stop the recoils, and correlate them

<sup>2</sup>Allegedly, Cranston discovered  $^{231}\text{Pa}$  already in 1915, but he was recruited to service at World War I, and had to delay the publication accordingly [22].

TABLE I. The beam energies ( $E_b^{\text{lab}}$ ), average beam intensities ( $I_b$ ), exposure times ( $t$ ), and the thicknesses of the target ( $d_T$ ) and the downstream carbon degrader foil ( $d_C$ ) used at different phases of this study.

Phase	Reaction	$E_b^{\text{lab}}$ (MeV)	$I_b$ (pnA)	$t$ (h)	$d_{\text{Ta}}$ ( $\mu\text{g}/\text{cm}^2$ )	$d_C$ ( $\mu\text{g}/\text{cm}^2$ )
1	$^{36}\text{Ar}+^{181}\text{Ta}$	178	141	8.2	1000	70
2	$^{36}\text{Ar}+^{181}\text{Ta}$	184	138	14.4	450	70
3	$^{36}\text{Ar}+^{181}\text{Ta}$	190	190	15.3	1000	70
4	$^{36}\text{Ar}+^{181}\text{Ta}$	196	196	20.9	1000	70
5	$^{36}\text{Ar}+^{181}\text{Ta}$	202	199	42.3	1000	70
6	$^{36}\text{Ar}+^{181}\text{Ta}$	208	210	68.8	1000	70
7	$^{36}\text{Ar}+^{181}\text{Ta}$	214	158	16.2	1000	70
8	$^{56}\text{Fe}+^{159}\text{Tb}$	274	76	19.0	1000	70
9	$^{56}\text{Fe}+^{159}\text{Tb}$	280	60	17.0	1000	70
10	$^{36}\text{Ar}+^{181}\text{Ta}$	210	180	80.6	1000	70

spatially with the subsequent characteristic  $\alpha$ -decay events. An event without the MWPC signal was considered as a decay. Decay chains including up to four consecutive  $\alpha$ -decay generations were searched for in the same pixel in the DSSD as that of the recoil implantation. Selection of such events is crucial in order to achieve a reliable identification as there are many overlapping  $\alpha$ -particle energies in the region, see the  $\alpha$ -particle energy spectrum displayed in Fig. 1(b). Furthermore, the detection efficiency of  $\alpha$  particles was enhanced with an array of 28 silicon PIN diodes, assembled in a tunnel geometry upstream of the DSSD, to detect  $\alpha$  particles escaping from the implantation detector. Data from all detector channels were timestamped with a 100 MHz clock, recorded independently, and analyzed using the GRAIN software package [37].

### III. RESULTS AND DISCUSSION

During this experiment, a total of 13 correlated  $\alpha$ -decay chains starting from protactinium isotopes were identified based on the previously known  $\alpha$ -decay properties of the daughter species. From these events, three represent the first rigorous observation of the new isotope  $^{211}\text{Pa}$ . From the remaining ten, seven were attributed to  $^{212}\text{Pa}$  and three to  $^{213}\text{Pa}$ . Previously, a total of only four decay events were assigned to  $^{212}\text{Pa}$  in Refs. [26,38], hence, the present experiment improved the published data. The isotope  $^{213}\text{Pa}$  was identified via five correlated  $\alpha$ -decay events in the Ref. [39], and that work, to our knowledge, remains the only published decay spectroscopy study of  $^{213}\text{Pa}$ . Therefore the present work provides important independent confirmation of the decay properties of  $^{213}\text{Pa}$ . It was estimated that less than 0.001 decay chains were recorded via random correlations over the full course of the experiment that has the  $\alpha$ -particle energy and decay time of the first and second decay matching to a real decay chain starting from any of the  $^{211,212,213}\text{Pa}$  isotopes. This number is further reduced if the third and fourth decay generation are considered.

The measured  $\alpha$ -particle energy and the decay-time distributions are displayed in Fig. 2, while the corresponding

numerical data are provided in the Appendix. The  $\alpha$ -particle energies and half-lives obtained from these decay chains are summarized in Table II together with a comparison to previously reported values, if available. Good agreement was found between the present results, and those of Refs. [26,38–40]. The half-lives were extracted with the exact maximum likelihood method described in Ref. [41] and the  $\alpha$ -particle energies were obtained as the arithmetic mean of the measured individual events. The extracted  $\alpha$ -decay energies are compared to those of AME2016 mass evaluation [42] in Fig. 3.

With the present data we extract the reduced  $\alpha$ -decay widths  $\delta^2$  via the method described by Rasmussen [43] assuming  $\alpha$  emission with  $l=0$  and an  $\alpha$ -decay branch of 100%<sup>3</sup>. Respective hindrance factors (HF) were obtained by normalizing the  $\delta^2$  values to those of the ground-state to ground-state decays of nearby even-even thorium isotopes; these results are given in Table II. As the hindrance factors are close to unity, the wave functions of the initial and final states of the  $\alpha$  decay are likely to overlap heavily. The  $\alpha$  decays of  $^{211,212,213}\text{Pa}$  correlate with the ground-state  $\alpha$  decay of the daughter nuclei  $^{207,208,209}\text{Ac}$ , whose ground states are proposed to have a spin and parity of  $(9/2^-)$ ,  $(3^+)$ , and  $(9/2^-)$  [2], respectively. Therefore, we propose an identical spin and parity pattern of  $(9/2^-)$ ,  $(3^+)$ , and  $(9/2^-)$  for the  $\alpha$ -decaying ground states in  $^{211,212,213}\text{Pa}$  isotopes, respectively. These states are likely to involve a contribution from an odd valence proton in the  $h_{9/2}$  orbital.

The present  $\alpha$ -decay energies can be used to probe the masses of the most exotic protactinium isotopes. This was done by adding the decay energy and the mass of the  $\alpha$  particle to that of the daughter nucleus (AME2016, [42]). Mass excesses  $\Delta$  obtained via this method are given in Table II together with the evaluated (AME2016) reference values. These mass excesses can then be used to extract the one- ( $S_p$ ) and two-proton separation energies ( $S_{2p}$ ), which are again listed in Table II, and compared to those of other nuclei in the region in Fig. 4. It is evident from Fig. 4, that the one-proton dripline has been reached for the protactinium and actinium isotopes, while the two-proton dripline for the more tightly bound even- $Z$  thorium isotopes is far beyond the lightest known isotope. Figure 4 also provides the predictions of selected mass models, namely KTUY05 [45], Liran-Zeldes [46], FRDM2012 [47], and the average of six energy-density functional based models (EDF [3], see Fig. 4 caption for further details). The EDF appear to reproduce reasonably well the experimental values of weakly bound ( $0 < S_p \lesssim 500$  keV) actinium and protactinium isotopes. It is also evident from Fig. 4 that all named mass models have a tendency to overpredict the  $S_p$  values of proton unbound actinium and protactinium isotopes. Good agreement is found for the  $S_{2p}$  of thorium isotopes through Liran-Zeldes shell-model calculations, but for the four cases shown, the finite-range droplet

<sup>3</sup>The quasiparticle random-phase approximation [44] predicts a  $\beta$ -decay half-life of  $\approx 1.8$  s for  $^{211}\text{Pa}$ , hence,  $\beta$  decay does not compete with the  $\alpha$ -particle emission. Possible proton emission is discussed later in this article.

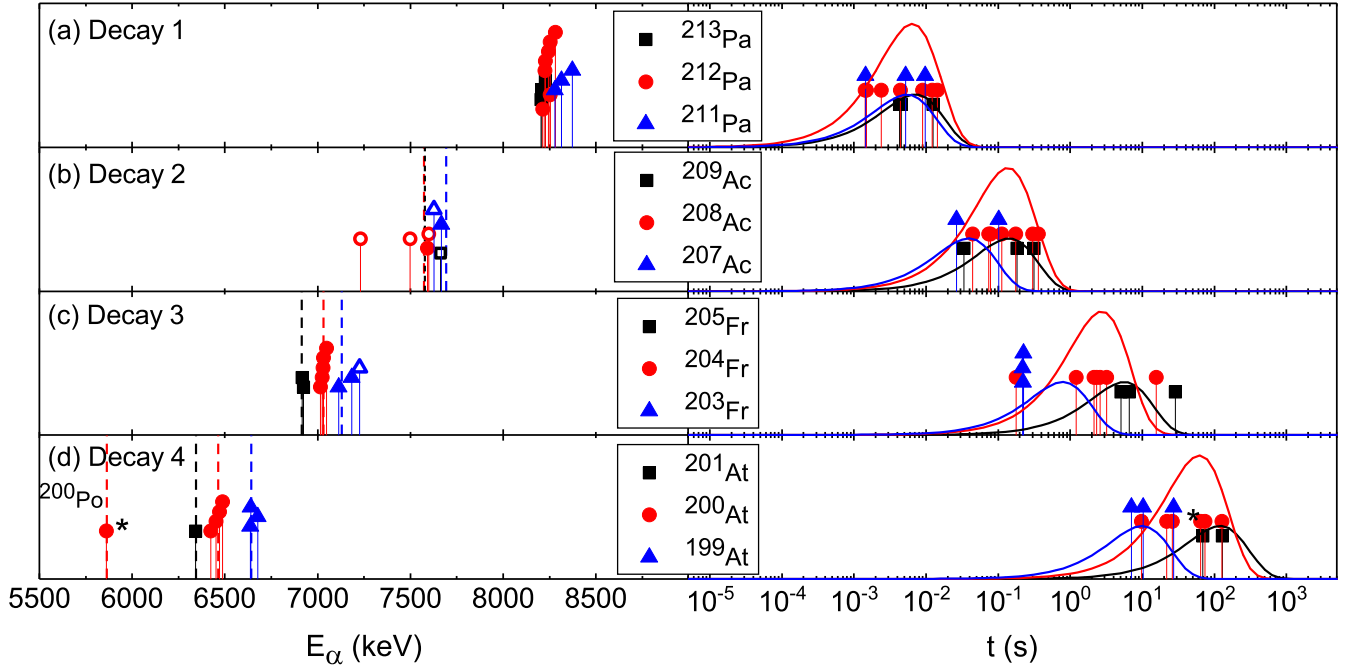


FIG. 2. The  $\alpha$ -particle energy and the decay-time distributions of the correlated  $\alpha$ -decay chains starting from the protactinium isotopes observed in the present study. The dashed lines on the left-hand side denote the literature values for the  $\alpha$ -particle energy of the given isotope, while the solid lines on the right-hand side are the decay-time probability density distributions corresponding to the extracted half-life (Decay 1) or to those given in the literature (Decays 2–4).  $\alpha$ -particle energies obtained from an escape event observed in the PIN diodes via an add-back procedure are indicated with hollow symbols. On the chain marked with an asterisk, a  $\beta^+$  decay or electron capture has occurred between the  $\alpha$  decays number 3 and 4, hence, the decay energy should be compared to that of  $^{200}\text{Po}$ , which is indicated with another dashed line. See also the Appendix for the numerical data of the individual decay events.

model (FRDM2012) of Möller *et al.* fits the data best. It predicts  $^{204}\text{Th}$  to be the first two-proton unbound isotope, most likely beyond the capabilities of the experimental techniques available to date.

As the  $S_p$  values of the  $^{211,212,213}\text{Pa}$  isotopes are negative, it is energetically plausible for them to spontaneously emit protons with  $^{211}\text{Pa}$  being the best candidate as it has the highest proton-decay energy. A thorough search through our data was conducted in order to identify the proton-decay

events of  $^{211}\text{Pa}$ , but no candidate events were found. This is not a surprise if we consider the situation via a simple WKB integral (Wentzel-Kramers-Brillouin). Assuming the present  $S_p(^{211}\text{Pa})$  value together with  $l = 5$  proton emission from the  $(9/2^-)$   $\pi h_{9/2}$  ground state of  $^{211}\text{Pa}$ , the WKB method predicts a partial proton-decay half-life of  $\sim 10^{16}$  s, far too slow to compete with the  $\alpha$ -particle disintegration. A robust extrapolation of  $S_p = a + bA^{-1/3} + cA^{-1}$ , arising from the liquid-drop model [48], to the  $S_p$  values of the few nearest even more

TABLE II. The properties of the protactinium isotopes obtained in this study, and those reported in the literature. Here, # indicates an extrapolated value, see the text for the definitions of the different quantities.

Quantity	$^{211}\text{Pa}$		$^{212}\text{Pa}$		$^{213}\text{Pa}$	
	Present	Literature	Present	Literature	Present	Literature
$T_{1/2}$ (ms)	$3.8^{+4.6}_{-1.4}$	—	$4.5^{+2.7}_{-1.3}$	$5.1^{+6.1}_{-1.9}$ [38] $5.1^{+5.1}_{-1.7}$ [26] <sup>a</sup>	$4.9^{+5.9}_{-1.8}$	$5.3^{+4.0}_{-1.6}$ [40]
$E_\alpha$ (keV)	8320(40)	—	8240(20)	8270(30) [38] 8250(20) [26] <sup>a</sup>	8210(20)	8236(15) [40]
$Q_\alpha$ (keV)	8480(40)	—	8400(20)	8430(30)	8370(20)	8394(15)
$\delta^2$ (keV)	35	—	48	—	51	—
$HF$	1.6	—	1.2	—	1.1	—
$\Delta$ (keV)	22050(60)	22080(100)# [42]	21570(70)	21590(70) [42]	19630(60)	19660(70) [42]
$S_p$ (keV)	−700(70)	−730(100)# [42]	−370(100)	−390(100) [42]	−230(60)	−260(70) [42]
$S_{2p}$ (keV)	1370(80)	1340(110)# [42]	1800(90)	1770(90) [42]	2150(80)	2120(90) [42]

<sup>a</sup>Authors of Ref. [26] obtained this value by combining their data with that of Ref. [38].

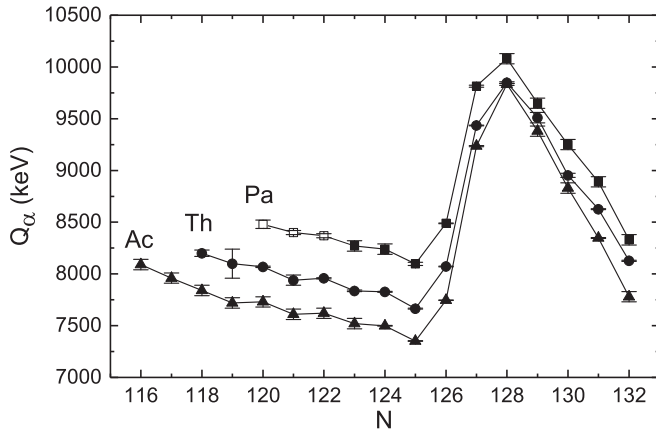


FIG. 3.  $\alpha$ -decay  $Q$  values obtained in this study (hollow symbols) compared to the systematics of the nearby isotopes (solid symbols, AME2016 [42]).

neutron-deficient protactinium isotopes reveals that in none of those the proton decay is able to compete with the  $\alpha$  decay, further widening the “Littoral shallow” of the nuclear instability.

The present  $S_p$  data allows us to address another intriguing question, the existence of the Thomas-Ehrman shift in heavy nuclei. This effect has been explained as a reduction of the repulsive Coulomb energy, arising from the fact that the wave functions of the valence protons span outside the nuclear interior in proton-unbound nuclei. In practice, one of the experimental signatures to look for is the difference between the measured and calculated charge-conjugate mass [56] of nuclei stable against proton emission, and compare to that

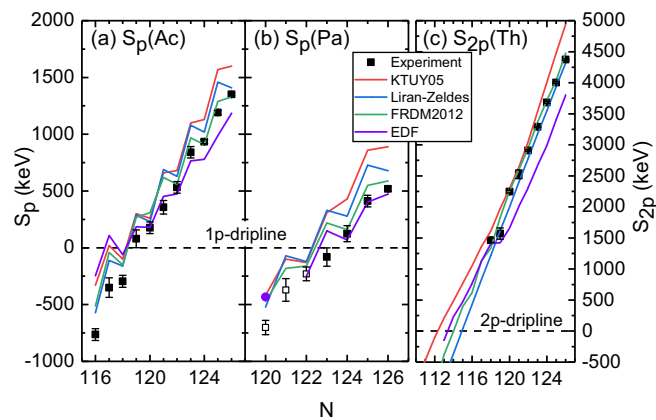


FIG. 4. One- [(a) actinium, (b) protactinium] and two-proton separation energies [(c) thorium] near the one-proton dripline. The experimental data points extracted from the mass-excesses of this study are indicated with the hollow symbols, while those of the atomic mass evaluation (AME2016, [42]) are given with solid symbols. Predictions of selected nuclear-mass models (Liran-Zeldes [46], FRDM2012 [47], and KTUY05 [45]) are plotted with solid lines. The line labeled EDF represents the average of six models [3] based on different energy-density functionals (SkM\* [49], SkP [50], SLy4 [51], SV-min [52], UNEDF0 [53], and UNEDF1 [54]). The EDF values were obtained using the *Mass explorer* interface [55].

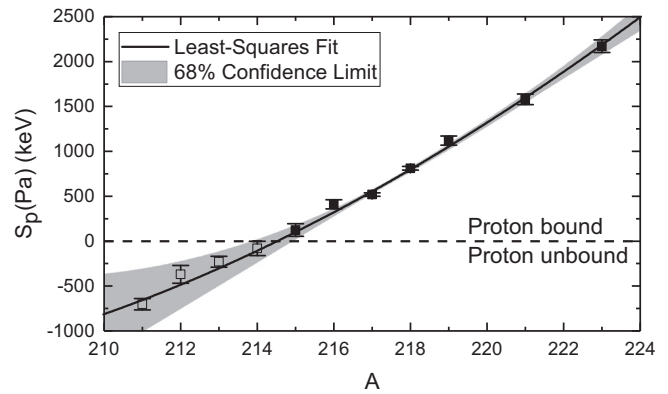


FIG. 5. One-proton separation energies of the protactinium isotopes obtained in this study, or in the AME2016 mass evaluation [42]. The solid line is a liquid-drop model fit to the proton bound data points (solid symbols), extrapolated over the region of the known isotopes beyond the proton dripline (hollow symbols). The shaded area indicates the uncertainties of the fitted function.

of proton-unstable nuclei. In Ref. [57], the Thomas-Ehrman shift was characterized for 11 beyond proton-dripline nuclei between  $^4\text{Li}$  and  $^{39}\text{Sc}$ , for which an average deviation between the experimental and the calculated masses of  $-576.5$  keV was obtained, in contrast to 3.4 keV of proton stable nuclei. Furthermore, in Ref. [58] Nazarewicz *et al.* showed that a significant Thomas-Ehrman shift is present in medium mass nuclei near the proton dripline. To address the effect in heavy nuclei we adopt the fitting procedure described in Ref. [48], i.e., we fit the liquid-drop model function quoted earlier to the proton bound  $S_p$  data, and look for an offset between the proton bound and the unbound nuclei. In Ref. [57] it was shown that the Thomas-Ehrman effect increases as a function of decreasing  $S_p$ , and therefore, it is worthy to repeat the analysis for the newly obtained data. The aforementioned least-squares fit is displayed in Fig. 5 and it shows a satisfactory agreement between the extrapolated fit and the measured  $S_p$  values of proton-unbound nuclei. An average deviation of 40(70) keV was found between the two, which does not provide statistically meaningful evidence on the Thomas-Ehrman shift in protactinium isotopes. As discussed in detail in Ref. [59], the effect is significant for unbound nuclei with low angular momentum. The ground states of the proton unbound protactinium isotopes are likely to involve a  $h_{9/2}$  valence proton, which does not favor the Thomas-Ehrman effect. From the point of view of low angular momentum, the  $1/2^+$  ground or isomeric state of  $\pi s_{1/2}$  spherical parentage observed in nearby bismuth (see, for example, Ref. [60] and references therein), astatine (Refs. [61–64]), and francium (Refs. [65–68]) nuclei might provide a better laboratory to identify the shift in heavy nuclei.

#### IV. SUMMARY

Using a fusion-evaporation reaction and a gas-filled recoil separator we have produced and, for the first time, identified rigorously the new isotope  $^{211}\text{Pa}$ . It was found to  $\alpha$  decay with a half-life and  $\alpha$ -particle energy of  $3.8^{+4.6}_{-1.4}$  ms and

TABLE III. Correlated  $\alpha$ -decay chains starting from the protactinium isotopes observed in this study. On the first column the events are numbered as they appear in the data, while the second one points to the experimental conditions of Table I.  $E_{\alpha n}$  and  $t_n$  are the measured  $\alpha$ -particle energy and decay time of the  $n$ th event on the decay chain, respectively. For comparison, the known  $\alpha$ -particle energies and half-lives of protactinium isotopes, and their subsequent decay products, are provided on the line labeled “Lit.” Decay energies reconstructed from an escape event caught by the PIN diodes are given in parentheses, while italics indicate a complete escape (no PIN signal present). On the chain number 7 a  $\beta^+$  or electron capture decay has occurred between the  $\alpha$  decays number 3 and 4, hence, the  $E_{\alpha 4}$  and  $t_4$  (marked with an asterisk) should be compared to those of  $^{200}\text{Po}$ , i.e., 5861.9(18) keV and 11.5(1) min [2], respectively.

Chain #	Phase	Parent isotope	$E_{\alpha 1}$ (keV)	$t_1$ (ms)	$E_{\alpha 2}$ (keV)	$t_2$ (ms)	$E_{\alpha 3}$ (keV)	$t_3$ (s)	$E_{\alpha 4}$ (keV)	$t_4$ (s)
Lit.		$^{213}\text{Pa}$	8236(15) [40]	$5.3^{+4.0}_{-1.6}$ [40]	7577(10) [40]	$98^{+59}_{-27}$ [40]	6915(1) [2]	3.92(4) [2]	6342(1) [2]	83(2) [2]
1	1	$^{213}\text{Pa}$	8209	4.31	407	184	6923	28.6	—	—
2	1	$^{213}\text{Pa}$	8227	4.52	(7663)	33.4	6917	6.60	6341	128.7
5	3	$^{213}\text{Pa}$	8205	12.5	355	313	2098	5.10	242	68.7
Lit.		$^{212}\text{Pa}$	8270(30) [38]	$5.1^{+6.1}_{-1.9}$ [38]	7572(15) [69]	$95^{+24}_{-16}$ [69]	7031(5) [2]	1.9(5) [2]	6464.6(13) [2]	43(1) [2]
3	3	$^{212}\text{Pa}$	8245	8.90	2413	78.0	742	2.60	6425	21.9
4	3	$^{212}\text{Pa}$	8224	1.49	(7499)	74.3	7032	0.18	6470	126.8
6	4	$^{212}\text{Pa}$	8254	4.44	1532	359	7030	3.19	6452	9.78
7	4	$^{212}\text{Pa}$	8213	1.44	(7599)	302	624	1.21	5862*	64.4*
8	4	$^{212}\text{Pa}$	8254	2.41	(7230)	112	7025	2.14	1742	74.6
9	4	$^{212}\text{Pa}$	8281	12.2	7593	175	7047	15.5	6487	26.2
10	4	$^{212}\text{Pa}$	8228	14.3	298	44.5	7015	2.31	—	—
Lit.		$^{211}\text{Pa}$	—	—	7693(25) [70]	$27^{+11}_{-6}$ [70]	7131(5) [2]	0.549(15) [2]	6643(3) [2]	6.92(13) [2]
11	5	$^{211}\text{Pa}$	8279	5.20	7667	103	(7227)	0.22	6637	27.1
12	5	$^{211}\text{Pa}$	8373	9.72	—	—	7185	0.22	6678	7.06
13	6	$^{211}\text{Pa}$	8314	1.46	(7626)	26.4	7114	0.23	6639	10.2

8320(40) keV, respectively, suggesting a favored  $\alpha$  decay. We also obtained more precise decay properties for the neighboring isotopes  $^{212}\text{Pa}$  and  $^{213}\text{Pa}$ . With these  $\alpha$ -decay data we improved the mass information of these three isotopes, and compared to the predictions of selected nuclear mass models via one-proton separation energies. Proton emission from these beyond-dripline nuclei was found unlikely. We also studied the Thomas-Ehrman shift in the light of the new one-proton separation energies, but no evidence of its presence in this mass region was found.

#### ACKNOWLEDGMENTS

This work was supported by the Academy of Finland under Contracts No. 213503 (Finnish Center of Excellence Pro-

gramme) and No. 323710 (personal research project, K.A.). The authors also thank the GAMMAPOOL European Spectroscopy Resource for the loan of the germanium detectors. The contribution of A.H. was supported by the Slovak Research and Development Agency (Contract No. APVV-15-0225), the Slovak grant agency VEGA (Contract No. 2/0129/17), and the project ITMS code no. 26210120023, supported by the Research and Development Operational Programme funded by ERDF (30%).

#### APPENDIX: $\alpha$ -DECAY DATA

The  $\alpha$ -particle energies and decay times measured for the decay chains starting from the protactinium isotopes are listed in Table III.

- [1] M. Thoennessen, Discovery of Nuclides Project webpage, accessed 04.02.2019, <https://people.nslc.msu.edu/~thoenness/isotopes/index.html>.
- [2] National Nuclear Data Center, Evaluated Nuclear Structure Data File, accessed via NUDAT 2.7 interface, <https://www.nndc.bnl.gov/nudat2/>.
- [3] J. Erler, N. Birge, M. Kortelainen, W. Nazarewicz, E. Olsen, A. M. Perhac, and M. Stoitsov, *Nature* **486**, 509 (2012).
- [4] H. Schatz, A. Aprahamian, V. Barnard, L. Bildsten, A. Cumming, M. Ouellette, T. Rauscher, F.-K. Thielemann, and M. Wiescher, *Phys. Rev. Lett.* **86**, 3471 (2001).
- [5] V. V. Elomaa, G. K. Vorobjev, A. Kankainen, L. Batist, S. Eliseev, T. Eronen, J. Hakala, A. Jokinen, I. D. Moore, Y. N. Novikov, H. Penttilä, A. Popov, S. Rahaman, J. Rissanen, A. Saastamoinen, H. Schatz, D. M. Seliverstov, C. Weber, and J. Äystö, *Phys. Rev. Lett.* **102**, 252501 (2009).
- [6] K. Auranen, D. Seweryniak, M. Albers, A. Ayangeakaa, S. Bottoni, M. Carpenter, C. Chiara, P. Copp, H. David, D. Doherty, J. Harker, C. Hoffman, R. Janssens, T. Khoo, S. Kuvin, T. Lauritsen, G. Lotay, A. Rogers, C. Scholey, J. Sethi, R. Talwar, W. Walters, P. Woods, and S. Zhu, *Phys. Lett. B* **792**, 187 (2019).
- [7] M. Arnould, S. Goriely, and K. Takahashi, *Phys. Rep.* **450**, 97 (2007).
- [8] C. J. Horowitz, A. Arcones, B. Côté, I. Dillmann, W. Nazarewicz, I. U. Roederer, H. Schatz, A. Aprahamian, D.

- Atanasov, A. Bauswein, T. C. Beers, J. Bliss, M. Brodeur, J. A. Clark, A. Frebel, F. Foucart, C. J. Hansen, O. Just, A. Kankainen, G. C. McLaughlin, J. M. Kelly, S. N. Liddick, D. M. Lee, J. Lippuner, D. Martin, J. Mendoza-Temis, B. D. Metzger, M. R. Mumpower, G. Perdikakis, J. Pereira, B. W. O'Shea, R. Reifarh, A. M. Rogers, D. M. Siegel, A. Spyrou, R. Surman, X. Tang, T. Uesaka, and M. Wang, *J. Phys. G: Nucl. Part. Phys.* **46**, 083001 (2019).
- [9] H. Yang, L. Ma, Z. Zhang, C. Yang, Z. Gan, M. Zhang, M. Huang, L. Yu, J. Jiang, Y. Tian, Y. Wang, J. Wang, Z. Liu, M. Liu, L. Duan, S. Zhou, Z. Ren, X. Zhou, H. Xu, and G. Xiao, *Phys. Lett. B* **777**, 212 (2018).
- [10] D. S. Ahn, N. Fukuda, H. Geissel, N. Inabe, N. Iwasa, T. Kubo, K. Kusaka, D. J. Morrissey, D. Murai, T. Nakamura, M. Ohtake, H. Otsu, H. Sato, B. M. Sherrill, Y. Shimizu, H. Suzuki, H. Takeda, O. B. Tarasov, H. Ueno, Y. Yanagisawa, and K. Yoshida, *Phys. Rev. Lett.* **123**, 212501 (2019).
- [11] G. Rosner, *Nucl. Phys. B* **167**, 77 (2007).
- [12] A. Gade, C. K. Gelbke, and T. Glasmacher, *Nucl. Phys. News* **24**, 28 (2014).
- [13] T. Motobayashi and H. Sakurai, *Prog. Theo. Exp. Phys.* **2012**, 03C001 (2012).
- [14] K. Auranen, D. Seweryniak, M. Albers, A. D. Ayangeakaa, S. Bottoni, M. P. Carpenter, C. J. Chiara, P. Copp, H. M. David, D. T. Doherty, J. Harker, C. R. Hoffman, R. V. F. Janssens, T. L. Khoo, S. A. Kuvin, T. Lauritsen, G. Lotay, A. M. Rogers, J. Sethi, C. Scholey, R. Talwar, W. B. Walters, P. J. Woods, and S. Zhu, *Phys. Rev. Lett.* **121**, 182501 (2018).
- [15] J. Hilton, J. Uusitalo, J. Sarén, R. D. Page, D. T. Joss, M. A. M. AlAqeel, H. Badran, A. D. Briscoe, T. Calverley, D. M. Cox, T. Grahn, A. Gredley, P. T. Greenlees, R. Harding, A. Herzan, E. Higgins, R. Julin, S. Juutinen, J. Konki, M. Labiche, M. Leino, M. C. Lewis, J. Ojala, J. Pakarinen, P. Papadakis, J. Partanen, P. Rahkila, P. Ruotsalainen, M. Sandzelius, C. Scholey, J. Sorri, L. Sottili, S. Stolze, and F. Wearing, *Phys. Rev. C* **100**, 014305 (2019).
- [16] H. Badran, C. Scholey, K. Auranen, T. Grahn, P. T. Greenlees, A. Herzan, U. Jakobsson, R. Julin, S. Juutinen, J. Konki, M. Leino, M. Mallaburn, J. Pakarinen, P. Papadakis, J. Partanen, P. Peura, P. Rahkila, M. Sandzelius, J. Sarén, J. Sorri, S. Stolze, and J. Uusitalo, *Phys. Rev. C* **94**, 054301 (2016).
- [17] Y. T. Oganessian, V. K. Utyonkov, Y. V. Lobanov, F. S. Abdullin, A. N. Polyakov, R. N. Sagaidak, I. V. Shirokovsky, Y. S. Tsyganov, A. A. Voinov, G. G. Gulbekian, S. L. Bogomolov, B. N. Gikal, A. N. Mezentsev, S. Iliev, V. G. Subbotin, A. M. Sukhov, K. Subotic, V. I. Zagrebaev, G. K. Vostokin, M. G. Itkis, K. J. Moody, J. B. Patin, D. A. Shaughnessy, M. A. Stoyer, N. J. Stoyer, P. A. Wilk, J. M. Kenneally, J. H. Landrum, J. F. Wild, and R. W. Lougheed, *Phys. Rev. C* **74**, 044602 (2006).
- [18] J. M. Gates, G. K. Pang, J. L. Pore, K. E. Gregorich, J. T. Kwargsick, G. Savard, N. E. Esker, M. Kireeff Covo, M. J. Mogannam, J. C. Batchelder, D. L. Bleuel, R. M. Clark, H. L. Crawford, P. Fallon, K. K. Hubbard, A. M. Hurst, I. T. Kolaja, A. O. Macchiavelli, C. Morse, R. Orford, L. Phair, and M. A. Stoyer, *Phys. Rev. Lett.* **121**, 222501 (2018).
- [19] R. G. Thomas, *Phys. Rev.* **88**, 1109 (1952).
- [20] J. B. Ehrman, *Phys. Rev.* **81**, 412 (1951).
- [21] K. Fajans and O. Göhring, *Naturwissenschaften* **1**, 339 (1913).
- [22] University of Glasgow webpage, Biography of John Arnold Cranston, accessed 07.02.2019, <https://universitystory.gla.ac.uk/biography/?id=WH3023&type=P>.
- [23] F. Soddy and J. A. Cranston, *Proc. R. Soc. London. Series A* **94**, 384 (1918).
- [24] O. Hahn and L. Meitner, *Phys. Z.* **19**, 208 (1918).
- [25] C. Fry and M. Thoennessen, *At Data Nucl. Data Tables* **99**, 345 (2013).
- [26] H. Yang, L. Ma, Z. Zhang, L. Yu, G. Jia, M. Huang, Z. Gan, T. Huang, G. Li, X. Wu, Y. Fang, Z. Wang, B. Gao, and W. Hua, *J. Phys. G: Nucl. Part. Phys.* **41**, 105104 (2014).
- [27] J. Kurcewicz, Z. Liu, M. Pfützner, P. Woods, C. Mazzocchi, K.-H. Schmidt, A. Kelić, F. Attallah, E. Badura, C. Davids, T. Davinson, J. Döring, H. Geissel, M. Górská, R. Grzywacz, M. Hellström, Z. Janas, M. Karny, A. Korgul, I. Mukha, C. Plettner, A. Robinson, E. Roeckl, K. Rykaczewski, K. Schmidt, D. Seweryniak, K. Sümmerer, and H. Weick, *Nucl. Phys. A* **767**, 1 (2006).
- [28] K. Rutz, M. Bender, P.-G. Reinhard, J. Maruhn, and W. Greiner, *Nucl. Phys. A* **634**, 67 (1998).
- [29] L. Geng, H. Toki, and J. Meng, *Prog. Theor. Phys.* **113**, 785 (2005).
- [30] E. Caurier, M. Rejmund, and H. Grawe, *Phys. Rev. C* **67**, 054310 (2003).
- [31] W. H. Long, H. Sagawa, N. V. Giai, and J. Meng, *Phys. Rev. C* **76**, 034314 (2007).
- [32] A. P. Leppänen, J. Uusitalo, M. Leino, S. Eeckhaudt, T. Grahn, P. T. Greenlees, P. Jones, R. Julin, S. Juutinen, H. Kettunen, P. Kuusiniemi, P. Nieminen, J. Pakarinen, P. Rahkila, C. Scholey, and G. Sletten, *Phys. Rev. C* **75**, 054307 (2007).
- [33] M. D. Sun, Z. Liu, T. H. Huang, W. Q. Zhang, J. G. Wang, X. Y. Liu, B. Ding, Z. G. Gan, L. Ma, H. B. Yang, Z. Y. Zhang, L. Yu, J. Jiang, K. L. Wang, Y. S. Wang, M. L. Liu, Z. H. Li, J. Li, X. Wang, H. Y. Lu, C. J. Lin, L. J. Sun, N. R. Ma, C. X. Yuan, W. Zuo, H. S. Xu, X. H. Zhou, G. Q. Xiao, C. Qi, and F. S. Zhang, *Phys. Lett. B* **771**, 303 (2017).
- [34] M. Leino, J. Äystö, T. Enqvist, P. Heikkinen, A. Jokinen, M. Nurmia, A. Ostrowski, W. Trzaska, J. Uusitalo, K. Eskola, P. Armbruster, and V. Ninov, *Nucl. Instrum. Methods Phys. Res. B* **99**, 653 (1995).
- [35] J. Sarén, J. Uusitalo, M. Leino, and J. Sorri, *Nucl. Instrum. Methods Phys. Res. A* **654**, 508 (2011).
- [36] R. Page, A. Andreyev, D. Appelbe, P. Butler, S. Freeman, P. Greenlees, R.-D. Herzberg, D. Jenkins, G. Jones, P. Jones, D. Joss, R. Julin, H. Kettunen, M. Leino, P. Rahkila, P. Regan, J. Simpson, J. Uusitalo, S. Vincent, and R. Wadsworth, *Nucl. Instrum. Methods Phys. Res. B* **204**, 634 (2003).
- [37] P. Rahkila, *Nucl. Instrum. Methods Phys. Res. A* **595**, 637 (2008).
- [38] S. Mitsuoka, H. Ikezoe, T. Ikuta, Y. Nagame, K. Tsukada, I. Nishinaka, Y. Oura, and Y. L. Zhao, *Phys. Rev. C* **55**, 1555 (1997).
- [39] V. Ninov, F. P. Heßberger, S. Hofmann, H. Folger, A. V. Yeremin, A. G. Popeko, A. N. Andreyev, and S. Saro, *Z. Phys. A: Hadrons Nucl.* **351**, 125 (1995).
- [40] F. P. Heßberger, S. Hofmann, D. Ackermann, V. Ninov, M. Leino, S. Saro, A. Andreyev, A. Lavrentev, A. G. Popeko, and A. V. Yeremin, *Euro. Phys. J. A* **8**, 521 (2000).

- [41] K. H. Schmidt, C. C. Sahn, K. Pielenz, and H. G. Clerc, *Z. Phys. A: At. Nucl.* **316**, 19 (1984).
- [42] M. Wang, G. Audi, F. G. Kondev, W. J. Huang, S. Naimi, and X. Xu, *Chin. Phys. C* **41**, 030003 (2017).
- [43] J. O. Rasmussen, *Phys. Rev.* **113**, 1593 (1959).
- [44] P. Möller, M. Mumpower, T. Kawano, and W. Myers, *At. Data Nucl. Data Tables* **125**, 1 (2019).
- [45] H. Koura, T. Tachibana, M. Uno, and M. Yamada, *Prog. Theor. Phys.* **113**, 305 (2005).
- [46] S. Liran and N. Zeldes, *At. Data Nucl. Data Tables* **17**, 431 (1976).
- [47] P. Möller, A. Sierk, T. Ichikawa, and H. Sagawa, *At. Data Nucl. Data Tables* **109–110**, 1 (2016).
- [48] Y. Novikov, F. Attallah, F. Bosch, M. Falch, H. Geissel, M. Hausmann, T. Kerscher, O. Klepper, H.-J. Kluge, C. Kozhuharov, Y. Litvinov, K. Löbner, G. Münzenberg, Z. Patyk, T. Radon, C. Scheidenberger, A. Wapstra, and H. Wollnik, *Nucl. Phys. A* **697**, 92 (2002).
- [49] J. Bartel, P. Quentin, M. Brack, C. Guet, and H.-B. Håkansson, *Nucl. Phys. A* **386**, 79 (1982).
- [50] J. Dobaczewski, H. Flocard, and J. Treiner, *Nucl. Phys. A* **422**, 103 (1984).
- [51] E. Chabanat, P. Bonche, P. Haensel, J. Meyer, and R. Schaeffer, *Nucl. Phys. A* **635**, 231 (1998).
- [52] P. Klüpfel, P.-G. Reinhard, T. J. Bürvenich, and J. A. Maruhn, *Phys. Rev. C* **79**, 034310 (2009).
- [53] M. Kortelainen, T. Lesinski, J. Moré, W. Nazarewicz, J. Sarich, N. Schunck, M. V. Stoitsov, and S. Wild, *Phys. Rev. C* **82**, 024313 (2010).
- [54] M. Kortelainen, J. McDonnell, W. Nazarewicz, P.-G. Reinhard, J. Sarich, N. Schunck, M. V. Stoitsov, and S. M. Wild, *Phys. Rev. C* **85**, 024304 (2012).
- [55] Michigan State University, Mass Explorer interface, <http://massexplorer.frib.msu.edu/>.
- [56] G. T. Garvey, W. J. Gerace, R. L. Jaffe, I. Talmi, and I. Kelson, *Rev. Mod. Phys.* **41**, S1 (1969).
- [57] E. Comay, I. Kelson, and A. Zidon, *Phys. Lett. B* **210**, 31 (1988).
- [58] W. Nazarewicz, J. Dobaczewski, T. R. Werner, J. A. Maruhn, P.-G. Reinhard, K. Rutz, C. R. Chinn, A. S. Umar, and M. R. Strayer, *Phys. Rev. C* **53**, 740 (1996).
- [59] S. Shlomo, *Rep. Prog. Phys.* **41**, 957 (1978).
- [60] A. N. Andreyev, D. Ackermann, F. P. Hessberger, K. Heyde, S. Hofmann, M. Huysse, D. Karlgren, I. Kojouharov, B. Kindler, B. Lommel, G. Münzenberg, R. D. Page, K. Van de Vel, P. Van Duppen, W. B. Walters, and R. Wyss, *Phys. Rev. C* **69**, 054308 (2004).
- [61] H. Kettunen, T. Enqvist, T. Grahn, P. Greenlees, P. Jones, R. Julin, S. Juutinen, A. Keenan, P. Kuusiniemi, M. Leino, A.-P. Leppänen, P. Nieminen, J. Pakarinen, P. Rakhila, and J. Uusitalo, *Eur. Phys. J. A* **17**, 537 (2003).
- [62] H. Kettunen, T. Enqvist, M. Leino, K. Eskola, P. Greenlees, K. Helariutta, P. Jones, R. Julin, S. Juutinen, H. Kankaanpää, H. Koivisto, P. Kuusiniemi, M. Muikku, P. Nieminen, P. Rakhila, and J. Uusitalo, *Eur. Phys. J. A* **16**, 457 (2003).
- [63] K. Auranen, J. Uusitalo, S. Juutinen, U. Jakobsson, T. Grahn, P. T. Greenlees, K. Hauschild, A. Herzán, R. Julin, J. Konki, M. Leino, J. Pakarinen, J. Partanen, P. Peura, P. Rakhila, P. Ruotsalainen, M. Sandzelius, J. Sarén, C. Scholey, J. Sorri, and S. Stolze, *Phys. Rev. C* **90**, 024310 (2014).
- [64] K. Auranen, J. Uusitalo, S. Juutinen, H. Badran, F. D. Bisso, D. Cox, T. Grahn, P. T. Greenlees, A. Herzán, U. Jakobsson, R. Julin, J. Konki, M. Leino, A. Lightfoot, M. Mallaburn, O. Neuvonen, J. Pakarinen, P. Papadakis, J. Partanen, P. Rakhila, M. Sandzelius, J. Sarén, C. Scholey, J. Sorri, and S. Stolze, *Phys. Rev. C* **95**, 044311 (2017).
- [65] J. Uusitalo, M. Leino, T. Enqvist, K. Eskola, T. Grahn, P. T. Greenlees, P. Jones, R. Julin, S. Juutinen, A. Keenan, H. Kettunen, H. Koivisto, P. Kuusiniemi, A.-P. Leppänen, P. Nieminen, J. Pakarinen, P. Rakhila, and C. Scholey, *Phys. Rev. C* **71**, 024306 (2005).
- [66] J. Uusitalo, J. Sarén, S. Juutinen, M. Leino, S. Eeckhaudt, T. Grahn, P. T. Greenlees, U. Jakobsson, P. Jones, R. Julin, S. Ketelhut, A.-P. Leppänen, M. Nyman, J. Pakarinen, P. Rakhila, C. Scholey, A. Semchenkov, J. Sorri, A. Steer, and M. Venhart, *Phys. Rev. C* **87**, 064304 (2013).
- [67] U. Jakobsson, S. Juutinen, J. Uusitalo, M. Leino, K. Auranen, T. Enqvist, P. T. Greenlees, K. Hauschild, P. Jones, R. Julin, S. Ketelhut, P. Kuusiniemi, M. Nyman, P. Peura, P. Rakhila, P. Ruotsalainen, J. Sarén, C. Scholey, and J. Sorri, *Phys. Rev. C* **87**, 054320 (2013).
- [68] K. Auranen, U. Jakobsson, H. Badran, T. Grahn, P. T. Greenlees, A. Herzán, R. Julin, S. Juutinen, J. Konki, M. Leino, A.-P. Leppänen, G. O'Neill, J. Pakarinen, P. Papadakis, J. Partanen, P. Rakhila, P. Ruotsalainen, M. Sandzelius, J. Sarén, C. Scholey, L. Sinclair, J. Sorri, S. Stolze, J. Uusitalo, and A. Voss, *Phys. Rev. C* **101**, 024306 (2020).
- [69] M. Leino, J. Uusitalo, T. Enqvist, K. Eskola, A. Jokinen, K. Loberg, W. Trzaska, and J. Äystö, *Z. Phys. A: Hadrons Nucl.* **348**, 151 (1994).
- [70] K. Eskola, P. Kuusiniemi, M. Leino, J. F. C. Cocks, T. Enqvist, S. Hurskanen, H. Kettunen, W. H. Trzaska, J. Uusitalo, R. G. Allatt, P. T. Greenlees, and R. D. Page, *Phys. Rev. C* **57**, 417 (1998).